46th Annual Review of Progress in Quantitative Nondestructive Evaluation
QNDE2019
July 14-19, 2019, Portland, OR, USA

QNDE2019-1234

A MODEL-BASED STUDY OF TRANSMIT-RECEIVE LONGITUDINAL ARRAYS FOR INSPECTION OF SUBSURFACE DEFECTS

Ehsan Mohseni[1], Charles Macleod, Yahsar Javadi, Zhen Qiu, Randika Vithanage, David Lines, Rastislav Zimermann, Gareth Pierce, Anthony Gachagan
Center for Ultrasonic Engineering
Department of Electronics and Electrical Engineering,
University of Strathclyde
Glasgow, UK

ABSTRACT

Dual matrix transmit-receive longitudinal arrays have been shown to have an improved signal to noise ratio in near field zone which makes them the most suitable array configuration for inspection of near surface defects. This study aims to compare the performance of different configurations for transmit-receive longitudinal matrix arrays. For this purpose, 4 matrix configurations of 2×32, 4×16, 4×32, and 8×16 elements are investigated using CIVA modelling. The array operating frequencies investigated are either 5 MHz or 10 MHz. Different natural focal depths for these TRL arrays are considered in the model. For each configuration, the ability to steer and skew the beam is examined through CIVA modelling of the inspection of flat bottom holes extended to a few millimeters under the surface. It is found that the focusing for near surface areas is more efficient using the 4×16 and 8×16 elements configurations.

Keywords: Transmit-receive longitudinal (TRL) matrix arrays, model-based ultrasonic studies, Non-destructive testing/evaluation, Matrix ultrasonic phased arrays

NOMENCLATURE

α	Separation angle between the matrix arrays
β	Depth of natural focus for TRL array

1. INTRODUCTION

Dual element longitudinal transmit-receive ultrasonic transducers were frequently used in the past to detect corrosion and perform wall thickness measurements in different industrial sectors [1]. These transducers were widely accepted by non-destructive testing community since the transmit-receive configuration minimizes the effect of the dead zone, resulting in an enhanced signal to noise ratio for near surface inspections [2]. Inspired by the same design, the idea was extended to ultrasonic arrays including linear and matrix arrays. These configurations, namely transmit-receive longitudinal (TRL) /shear (TRS) arrays, were soon adopted by the welding and joining community because of their increased sensitivity in noisy materials, such as austenitic stainless steels, relative to structural steels [3, 4]. Moreover, as another advantage of TRL/TRS arrays, the ability to steer the beam in two-directions can be named [5]. However, in weld applications the inspections are majorly done by high angle beams and the probe's distance from the weld zone is reasonably larger than the near field zone associated to each array [6]. Hence, the previous studies fall short when it comes to the performance of such arrays for detection of near surface defects.

The present study investigates the sensitivity of TRL arrays in detection of defects that lie sub-surface (*i.e.* up to 20 mm deep under the surface). For this purpose, CIVA is used to model different configurations of TRL matrix arrays and their performance in detection of near surface defects. Here, as demonstrated in Figure 1, the term performance stands for the ability to focus the probe's beam in close proximity to the material front surface, beam steering in primary inspection plane (*i.e.* the plane aligned with the length of the array), and beam skewing in the secondary inspection plane (*i.e.* the transversal plane with respect to the array's length). To address these, four TRL probes, all having a zero-degree stand-off from the material surface, are considered in the study. However, this abstract only discusses the results of two arrays of 2×32 and 4×16 in summary.

[1] Contact author: ehsan.mohseni@strath.ac.uk

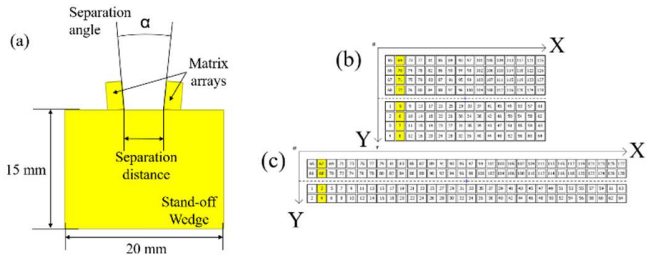

FIGURE 2: (a) ASSEMBLY OF THE STAND-OFF WEDGE AND MATRIX ARRAYS, AND LAYOUT FOR 64 CHANNELS TRANSMIT AND ARECEIVE MATRIX ARRAYS OF (b) 2×32, AND (c) 4×16.

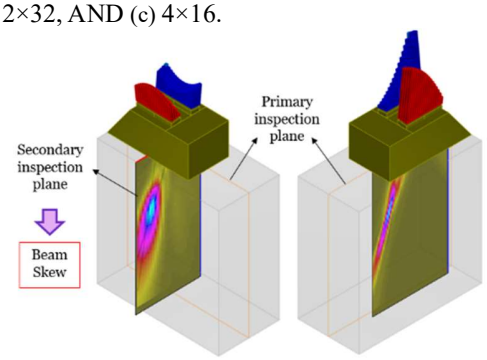

FIGURE 1: BEAM STEERING AND SKEWING IN THE PRIMARY AND SECONDARY INSPECTION PLANES, RESPECTIVELY

2. MATERIALS AND METHODS

A number of matrix arrays on a stand-off wedge, made out of Rexolite, with dimensions of 40 mm×20 mm×15 mm is prepared in CIVA. As depicted in Figure 2(a), there is a separation angle and distance between the two arrays mounted on the wedge, which can affect the quality of the beam focusing. Therefore, to conduct the study, the separation angle (α) is varied in a manner to have a natural beam focus (β) at 5 mm, 10 mm, and 15 mm under the interface of the wedge and the material while the separation distance is fixed at 5 mm. Four different matrix layouts of 2×32, 4×16, 4×32, and 8×16 elements are designed where the first two operate at 5 MHz and have 64 channels in transmit and receive, as can be seen in Figure 2(b). In the present example, the arrays have square elements with size of 1 mm with a separation of 0.1 mm in both matrix dimensions. The other two arrays are tested at frequency of 10 MHz. They have 128 channels of transmit and receive and their elements are 0.3 mm square with a separation of 0.1 mm in both directions of the matrix. It should be noted that these element sizes are only used for the preliminary study, and the final submission also discusses rectangular elements.

A titanium block with dimensions of 100×60×30 mm is placed beneath the wedge and arrays assembly. In the first stage of simulations, the block does not contain any defects since the aim is to investigate the effect of different β values on the ability of electronic beam focusing at different depths. α angle is set to have natural focus (β) at depths of 5 mm, 10 mm, 15 mm, and 20mm. Afterwards, for each β value, focal laws are changed to electronically focus the beam at different depths starting from 1 mm to 20 mm with increments of 1 mm.

In second stage of the study, a titanium block containing flat bottom holes (FBH) is defined. These holes extend from the lower surface of the block at different depths under the wedge/block interface. The distance from the wedge/block interface to the tip of the hole is changed from 3 mm to 30 mm with increments of 3 mm. The holes' centerline relative to the wedge center point is changed to compare the FBH indications for different matrix configurations, steering angles, and skew angles. These different positions are named and listed as follows:

1) In-plane centered: The FBH's centerline is centered with the wedge to get an insight into the effectiveness of multi-depth focusing for different matrix configurations. Wedge is placed on each hole to carry out the inspection as demonstrated in Figure 3(a).
2) In-plane with offset: All FBHs are located in the primary inspection plane, referring to Figure 3(b). Subsequently, each of these holes is inspected by positioning the wedge in a way that its center point is 5 mm away from the hole's centerline.
3) Out of plane: FBHs are offset by 5 mm from the primary inspection plane. This setup, as depicted in Figure 3(c) is meant for studying the ability of beam skewing.

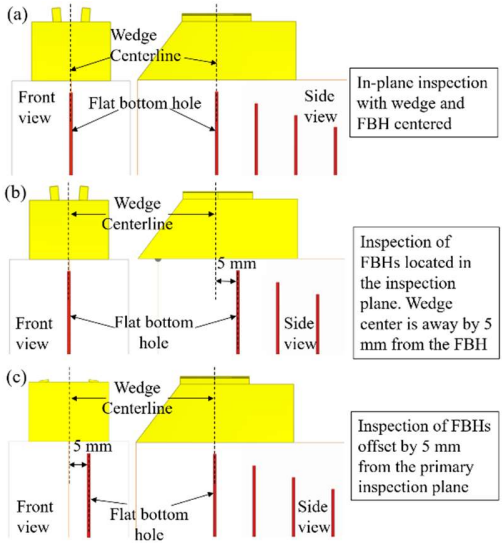

FIGURE 3: POSITIONING OF THE WEDGE WITH RESPECT TO THE FLAT BOTTOM HOLES IN THE SETUP PREPARED TO STUDY (a) MULTI-DEPTH FOCUSING, (b) BEAM STEERING, AND (c) BEAM SKEWING.

3. RESULTS AND DISCUSSION

Figures 4(a) and (b) plot the results of the study of beam focusing for two arrays of 2×32 and 4×16, respectively. It should be noted that the amplitude levels presented in Figure 4(a) cannot be compared to those in Figure 4(b) since there is not a possibility to normalize the amplitude values of one study to

another when using the beam computation module in CIVA. In these figures, although the depth focusing increments are 1 mm, but the actual position of the focal point doesn't always match the adjusted focal depth. For instance, according to Figure 4(b), the maximum amplitude of the focal spot falls at the position of 17.3 mm under the wedge/block interface when the beam of a 4×16 TRL array is focused at the depth of 20 mm. The discrepancies between the nominal and actual focusing point increase as the beam is focused deeper into the material. Moreover, the difference is higher when one uses a 4×16 array.

These figures also imply that the graph shifts forward for each array as the natural focal depth increases from 5 to 20 mm; however, this displacement is not significant. As an example, the amplitude for a beam focused at 15 mm using a 4×16 array increases by 2 dB as the natural focus is changed from 5 to 20 mm. It is notable that the maximum beam amplitude always falls at a depth of 5 mm for both arrays, regardless of the natural focus (*i.e.* β value). These graphs also show that the beam energy falls by 10 dB as the focus moves from 5 mm to 20 mm for 4×16 matrix array. It is safe to say that the focusing performance of the 4×16 array drops rapidly as the beam is focused at deeper areas whereas the performance of a 2×32 is predicted to be more consistent. To understand this better, Figure 5 presents the comparison between the shape of focal spot for the two arrays of 2×32 and 4×16, as the focusing depth changes from 3 mm to 21 mm with steps of 6 mm and the natural focus is kept at 10 mm.

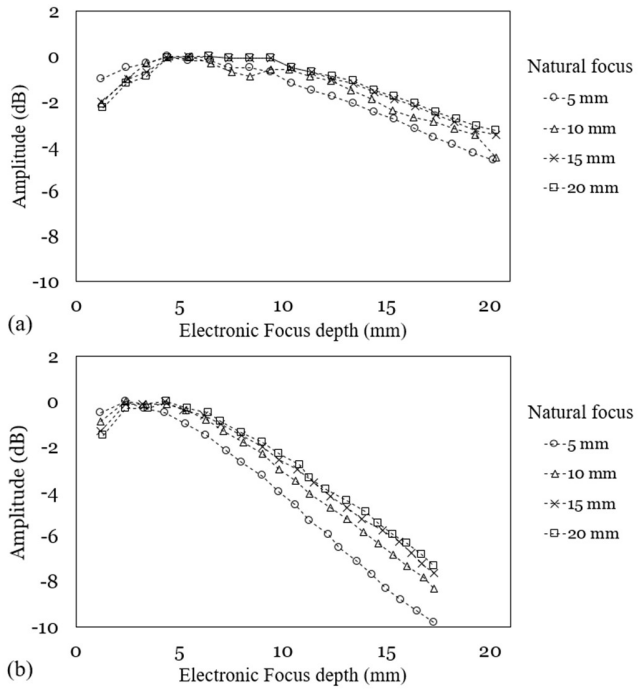

FIGURE 4: VARIATIONS OF THE MAXIMUM AMPLITUDE OF THE FOCAL SPOT VERSUS THE FOCUSING DEPTH FOR (a) A 2×32 MATRIX ARRAY, AND (b) A 4×16 MATRIX ARRAY

Figure 5 clearly demonstrates the change of amplitude for a 4×16 array as the beam is focused in deeper areas. It is also interesting that the focal spot of a 4×16 array is mainly extended through depth whereas the oval shaped focal spot of a 2×32 has its main axis along the horizontal direction.

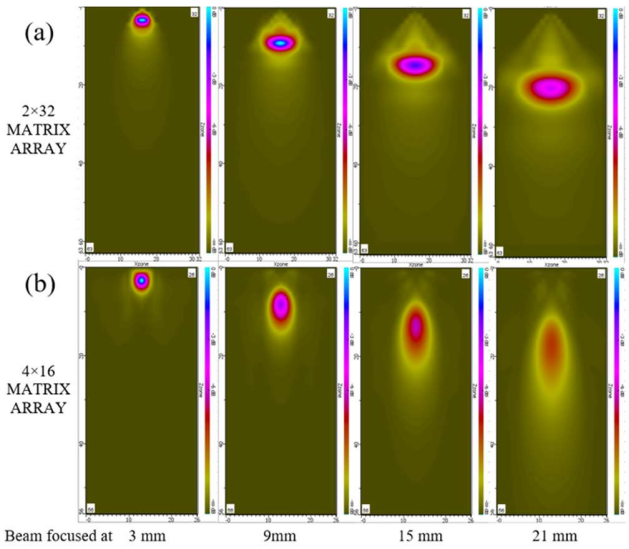

FIGURE 5: CHANGES IN THE SHAPE OF FOCAL SPOT AS THE ELECTRONIC FOCUS VARIES FROM DEPTH OF 3 MM TO 21 MM IN 4 STEPS FOR (a) A 2×32 MATRIX ARRAY, AND (b) A 4×16 MATRIX ARRAY.

The results concerning the second part of this study for 4×16 and 2×32 arrays are presented in Figure 6. The amplitude variations are plotted versus the distance of the hole from the wedge/block interface for two types of FBHs; (1) all FBHs located in the inspection plane, and (2) FBHs are offset by 5 mm from the inspection plane. All the amplitude computations are normalized to the amplitude of an in-inspection plane FBH located at 3 mm under the surface and measured by a 4×16 array.

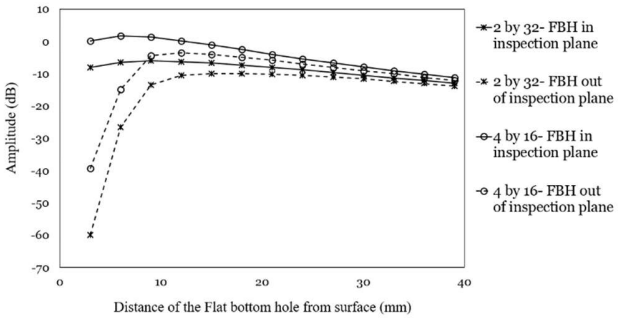

FIGURE 6: AMPLITUDE OF FLAT BOTTOM HOLES LOCATED AT DIFFERENT DEPTHS UNDER THE WEDGE/BLOCK INTERFACE. INSPECTIONS USING TWO TRL MATRIX ARRAYS OF 2×32 AND 4×16

According to the graphs presented in Figure 6, it is very unlikely to detect defects located at depths up to 9 mm using beam skewing when the holes are out of the inspection plane.

Looking at the signal of holes located in the inspection plane, it can be concluded the signal amplitude is the highest for the holes falling between the depth of 5 to 10 mm. It is clear that the indication's amplitude reduces due to attenuation as the inspection is done for deeper holes. In general, the signal amplitude for FBHs recorded by 4×16 appears to be always higher, regardless of the depth being inspected. These results are useful when one considers to design arrays that provide high detection probabilities.

4. CONCLUSION

For arrays with 64 elements, it is found that a matrix array with closer number of elements across X and Y directions has a superior performance particularly in proximity to the inspection surface. It is also observed that the beam skewing is not very efficient up to a depth of 10 mm no matter which configuration is selected. The simulation results suggest that the change of the separation angle between the transmit and receive matrixes doesn't have any significant influence on the energy of the focal point up to 20 mm deep into material. The present abstract only summarizes the results of the study for arrays of 64 channels. Those with 128 channels will be discussed in the presentation and the final manuscript.

REFERENCES

[1] Lebowitz, Carol A., and Lawrence M. Brown. "Ultrasonic measurement of pipe thickness." In *Review of Progress in Quantitative Nondestructive Evaluation*, pp. 1987-1994. Springer, Boston, MA, 1993.

[2] Kaczmarek, R. and Kaczmarek, K., 2016. The influence of sensitivity field of dual transducer probes on accuracy of discontinuity sizing and evaluation in terms of testing of forgings according to en 10228-3. *Archives of Metallurgy and Materials*, *61*(3), pp.1677-1682.

[3] Juengert, A., Dugan, S., Homann, T., Mitzscherling, S., Prager, J., Pudovikov, S. and Schwender, T., 2018, April. Advanced ultrasonic techniques for nondestructive testing of austenitic and dissimilar welds in nuclear facilities. In *AIP Conference Proceedings* (Vol. 1949, No. 1, p. 110002). AIP Publishing.

[4] Dombret, P., 1991. Methodology for the ultrasonic testing of austenitic stainless steel. *Nuclear engineering and design*, *131*(3), pp.279-284.

[5] Russell, J., R. Long, D. Duxbury, and P. Cawley. "Development and implementation of a membrane-coupled conformable array transducer for use in the nuclear industry." *Insight-Non-Destructive Testing and Condition Monitoring* 54, no. 7 (2012): 386-393.

[6] Nageswaran, C. and Bird, C.R., 2008. Evaluation of the phased array transmit-receive longitudinal and time-of-flight diffraction techniques for inspection of a dissimilar weld. *Insight-Non-Destructive Testing and Condition Monitoring*, *50*(12), pp.678-684.